Secondary Structure in Solution of Barwin from Barley Seed Using ^1H Nuclear Magnetic Resonance Spectroscopy

Svend Ludvigsen‡ and Flemming M. Poulsen*

Carlsberg Laboratorium, Kemisk Afdeling, Gamle Carlsberg Vej 10, DK-2500 Valby, Copenhagen, Denmark

Received November 27, 1991; Revised Manuscript Received June 9, 1992

ABSTRACT: Barwin, a basic protein from barley seed of 125 amino acid residues, has been studied by two-dimensional ^1H nuclear magnetic resonance spectroscopy. This protein is closely related to the C-terminal domain of proteins whose synthesis is induced by wounding, the so-called *win* proteins. These proteins may, therefore, have a role in the defense against fungal attack. Full assignment of the ^1H nuclear magnetic resonances has been obtained for 104 amino acid residues, and 18 amino acid spin systems were partially assigned. Sequence-specific assignment using nuclear Overhauser spectroscopy has been achieved for 122 of the 125 residues. This has revealed that the secondary structure of the protein is dominated by a large four-stranded antiparallel β-sheet consisting of the strands Gln2–Thr9, Lys65–Asn71, Gln77–Arg81, and His113–Val121, a small parallel β-sheet of the strands Trp48–Cys52 and Asp84–Ala87, which together account for a third of the protein. Sequential effects indicate the presence of three small α-helices, Tyr30–Lys38, Leu40–Tyr46, and Thr97–Asp103. The secondary structure in other regions of the sequence is characterized mainly by loops and turns and regions where no regular secondary structure arrangement could be identified. A large number of long-range nulcear Overhauser effects has been identified, and these have been used, together with sequential and intranuclear Overhauser effects, for a calculation of the protein's three-dimensional structure.

Plants possess a large variety of defense systems. These are often proteins directed against specific targets, as, for example, the ribosome inhibiting proteins (RIPs) that inhibit protein synthesis in the infecting organism, the proteinase inhibitors that act on foreign proteinases, or chitinases that digest the chitin cell walls of intruding fungi. Recently it was demonstrated that the synthesis of certain proteins that are related to chitin-binding proteins was induced by wounding of the plant cell (Stanford et al., 1989; Broekaert et al., 1990). At the time of these observations hevein of rubber tree was the only known protein of the type produced as a consequence of wounding. Hevein, however, only constitutes an N-terminal domain of the entire *win* protein. No C-terminal domain of the *win* protein has so far been isolated from plant sources, and just recently one of these protein domains was expressed in *Escherichia coli* (Lee et al., 1991) using recombinant gene methods. From barley seed, however, we have isolated a protein that is very closely related to the C-terminal part of the wound-induced protein in potato and rubber tree (Svensson et al., 1992).

Given that these proteins seem to be common in plants and have highly conserved sequences, a study of the three-dimensional structure of one of these can provide a structural platform for the elucidation of related structures and for the study of their function. The obvious interest in the natural defense systems of plants and their implications for plant health make a study of the three-dimensional structure of these proteins relevant, even before we know their specific function in the plants.

The present work is the second in a series of papers describing our studies aimed to determine the three-dimensional structure of barwin[1] in solution using two-dimensional ^1H NMR spectroscopy. Here we report the sequence-specific assignment of the NMR spectra of this protein and the secondary structure that has been determined on the basis of these assignments, sequential NOEs, and measurements of $^3J_{H^NH^\alpha}$ coupling constants. The following paper (Ludvigsen & Poulsen, 1992) describes the three-dimensional solution structure of barwin. Previously we have described the amino acid sequence and the homology with *win* proteins (Svensson et al., 1992).

MATERIALS AND METHODS

Samples of barwin for NMR recordings were prepared to make a 3 mM protein solution by dissolving 25 mg of the protein in 600 μL of solvent, which was either 99.96% ^2H_2O or a 19/1 (v/v) mixture of $H_2O/^2H_2O$ and adjusted to pH 4.20 or 7.00. In both cases the pH-meter readings were recorded, and no correction for deuterium effects was applied. Deuterium oxide was purchased from Merck.

NMR spectra were recorded on a Bruker AM500 NMR spectrometer equipped with an Aspect 3000 computer. The following two-dimensional NMR experiments were performed: NOESY (Jeener et al., 1979; Anil-Kumar et al., 1980, 1981; States et al., 1982), COSY (Aue et al., 1976; Marion & Wüthrich, 1983; Neuhaus et al., 1985), DQF-COSY (Piantini et al., 1982; Rance et al., 1983), relayed COSY (Eich et al., 1982; Wagner, 1983), 2QS (Boyd et al., 1983; Braunschweiler et al., 1983; Wagner & Zuiderweg, 1983), and TOCSY (Braunschweiler & Ernst, 1983; Bax et al., 1985; Griesinger et al., 1988). In all cases the spectra were recorded and transformed according to the method of States et al. (1982), yielding quadrature detection in ω_1 and pure phases (Bach-

* Author to whom correspondence should be addressed.
‡ Present address: Novo Research Institute, Novo Nordisk, Novo Allé, DK-2880 Bagsværd, Copenhagen, Denmark.

[1] Abbreviations: NOESY, two-dimensional nuclear Overhauser enhanced spectroscopy; COSY, two-dimensional correlated spectroscopy; DQF, double quantum filtered; TOCSY, total correlation spectroscopy; 2QS, double quantum spectroscopy; barwin, basic protein from barley seed.

0006-2960/92/0431-8771$03.00/0 © 1992 American Chemical Society

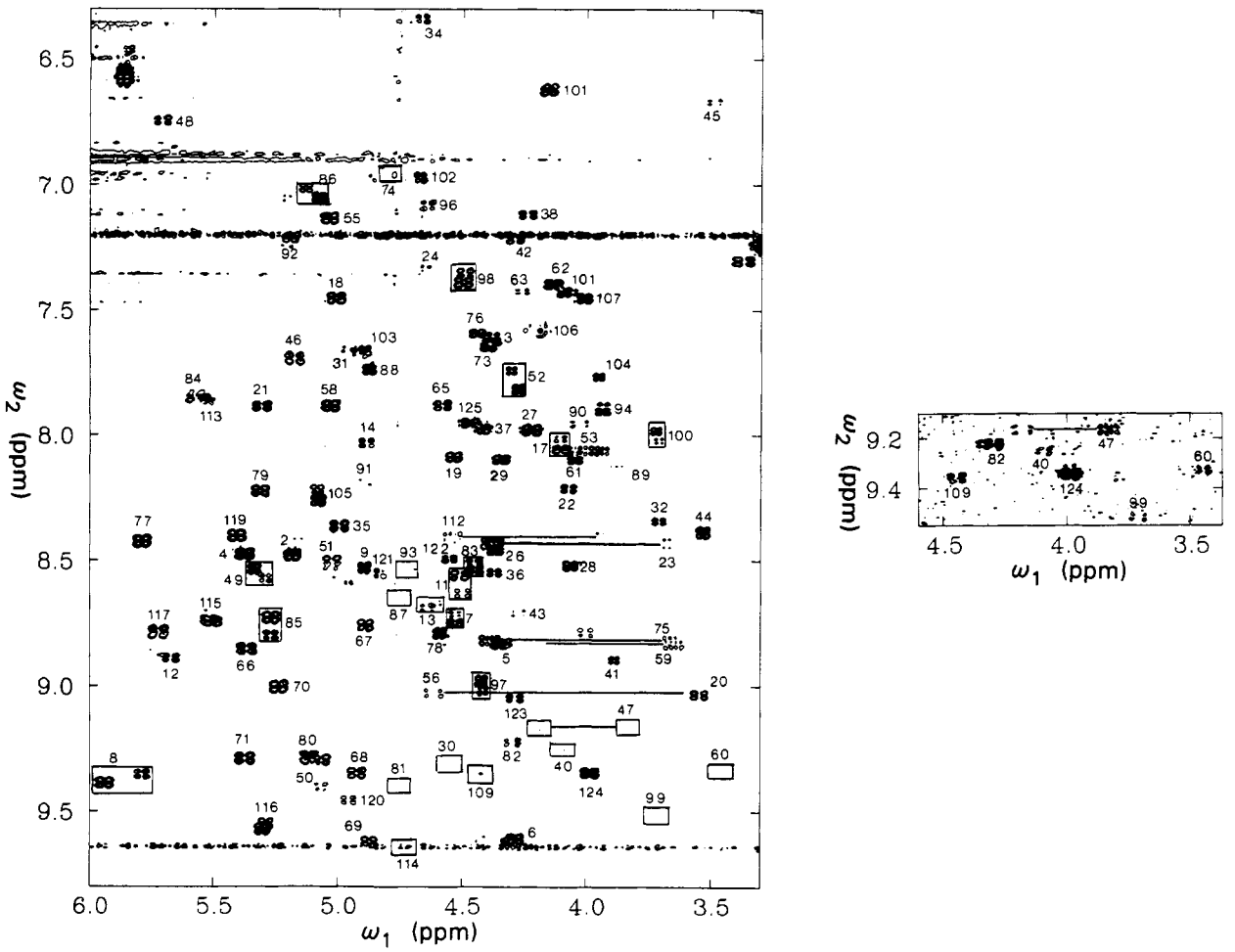

FIGURE 1: (a, left) Fingerprint region of the COSY spectrum of barwin, 3 mM in 1/19 $H_2O/^2H_2O$, at pH 4.20 and 310 K. Cross peaks are labeled with their residue number. The H^N–H^α cross peaks of residues Tyr10, Ala16, Thr33, Gly108, and Tyr118 are outside the plotted region. H^N–H^α cross peaks of Tyr30, Leu40, Gly47, Gln60, and Thr99 are not intense enough to be seen at these contour levels. All of these are shown with lower contours of a small part of the fingerprint region in (b). Thr74, Leu93, Ala87, Arg81, and Leu114 are buried in the water resonance. For these cross peaks boxes indicate their position in the fingerprint region. Several of the glycine cross peaks are connected by a horizontal line. Pairs of boxed cross peaks refer to the presence of two conformers (see text). (b, right) Part of fingerprint region in (a) but plotted with lower contours.

mann et al., 1977). For spectra in pure ^2H_2O the spectral width was 6097.5 Hz, and for spectra in 1/19 $^2H_2O/H_2O$ it was 6493.5 Hz, thus covering a little more than 100 Hz of the extreme chemical shift value present in barwin in both cases. For all spectra 1024 FIDs of 2048 complex points were recorded, corresponding to 512 complex points in the t_1 dimension. For each FID 64 scans and 2 dummy scans were recorded, with a relaxation delay of 1 s between scans. Mixing times of 50, 100, 150, and 200 ms were used for NOESY experiments. All assignments of NOESY spectra were based on spectra with mixing times of 150 ms. The data were transferred to a Stardent 1500 or SGI personal IRIS for all further processing using a software processing package developed in our laboratory (Kjær and Andersen, unpublished data). After zero filling to a 2K by 2K complex data matrix and after applying a negative line broadening of 9 Hz combined with a Gaussian line broadening of 12 Hz in t_2 and a squared sine bell shifted $\pi/2.6$ in t_1, the spectra were Fourier transformed.

Assignment of the spectra was acheived partly by manual analysis and lately by using the protein assignment program Pronto (Kjær et al., 1991). Integration of NOESY cross peaks was performed in this program. A rectangular area around each cross peak was selected either manually or automatically, and subsequently all data points in this area were added after a local baseplane correction. Intensities of NOESY cross peaks were classified as either strong, medium, or weak on the basis of integrations of the 100- and 150-ms mixing time NOESY spectra. When overlap occurred, the cross peaks were most often classified as weak if no reasonable judgment of the intensity could be made. The $^3J_{H^NH^\alpha}$ coupling constants were measured as described by Ludvigsen et al. (1991) using a combined analysis of NOESY and COSY spectra which usually were transformed for this purpose in a 4K by 2K data matrix to get a better resolution in ω_2. Contour diagrams of the spectra were produced for assignments after baseline corrections using either Legendre polynomials or the method reported by Dietrich et al. (1991) along ω_2.

RESULTS

The assignments of the NMR spectra of barwin were based on the analysis of several sets of two-dimensional ^1H NMR spectra including NOESY, COSY, relayed COSY, TOCSY, and 2QS spectra recorded at pH 7.0 or 4.2 and at several temperatures between 300 and 330 K. However, the best spectra were those obtained at 310 K and pH 4.2, where the amide exchange is slow and the optimal suppression of the water resonance could be achieved. At higher temperatures the protein was only stable for a short period, and at low temperatures the full suppression of the water resonance was difficult. Therefore, all reported chemical shift values are at 310 K and pH 4.20, but spectra at other conditions were used to resolve overlap of resonances.

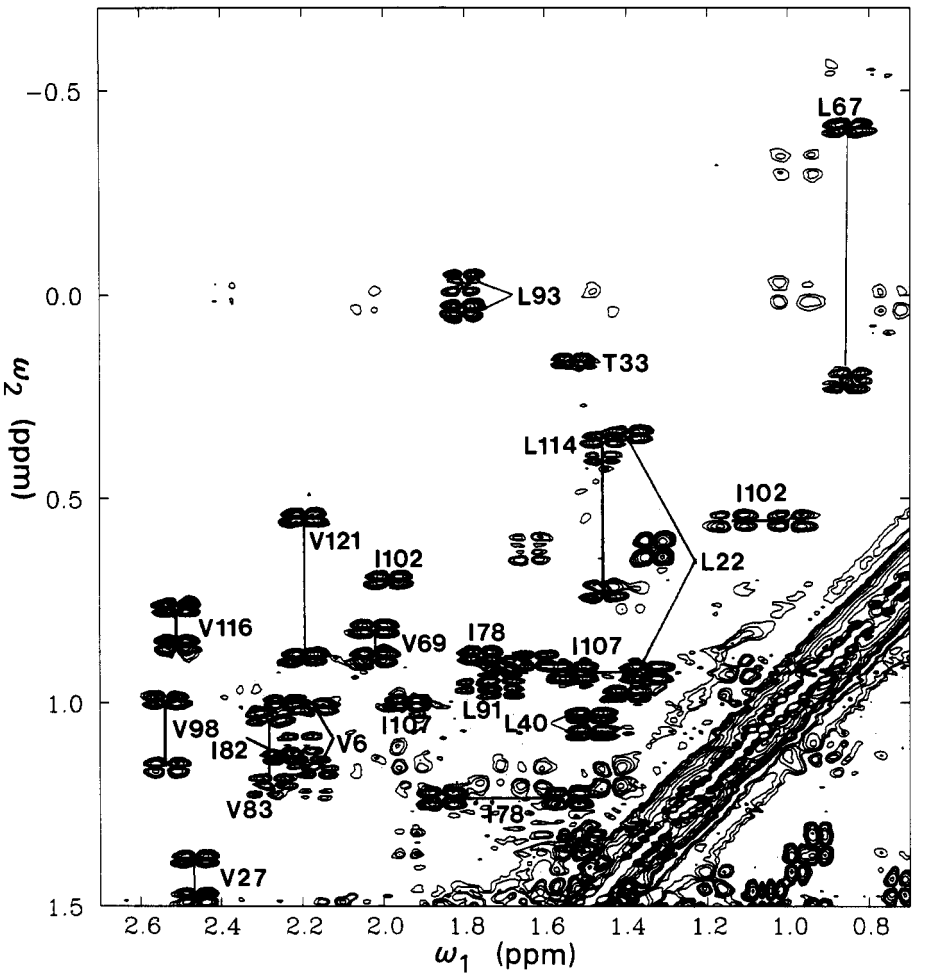

FIGURE 2: Part of DQF-COSY showing all valine, leucine, and isoleucine cross peaks including methyl groups. The spectrum is recorded under the same conditions as those in Figure 1. The solvent used is 99.96% ^2H_2O.

The methods of assignments have followed very closely the guidelines already well established in studies of many other proteins in the size range up to 10 000 Da (Wüthrich, 1986). Some spin systems could be identified immediately; these were glycines, alanines, threonines, isoleucines, and valines. Other spin systems were classified either as AMX spin systems (tryptophans, tyrosines, phenylalanines, histidines, asparagines, aspartates, cysteines, and serines) or as long side chain spin systems (leucines, lysines, arginines, prolines, and glutamines). There are no methionines or glutamates in the barwin sequence. In the following all spin systems are named by their sequential position even though the actual sequential assignment was not achieved in the first stage of the assignment process.

Fingerprint Region. The initial analysis of the fingerprint region of the COSY spectrum of barwin (Figure 1) revealed more H^N–H^α cross peaks than accounted for by the sequence. It was, however, soon realized that several of the residues were represented by two slightly separated cross peaks in the fingerprint region. At higher temperatures some of these pairs of cross peaks collapsed into one; however, a full analysis of this phenomenon was hampered by the lability of the protein at higher temperatures. The temperature dependence of this double-cross-peak phenomenon suggests that the protein exists in a two-stage conformational equilibrium at 310 K. However, no chemical exchange cross peaks between atoms in the two forms have been observed to indicate an equilibrium between the two forms. These observations will be discussed in detail later. The ratio between the two forms of the protein was estimated to be 1:3. Some of the cross peaks were, however, of very low intensity and therefore not visible in Figure 1. No H^N–H^α cross peaks have been seen for Gly64, Trp95, and Gln111 in the fingerprint region, and one cross peak has not been assigned. Some H^N–H^α cross peaks are located outside the shown region; these are Tyr10, Ala16, Thr33, Gly108, and Tyr118. Arg81 was only observed in the spectra of barwin dissolved in 99.96% ^2H_2O.

Amino Acid Spin System Assignments. Glycines (12 at Sequence Positions 23, 47, 53, 56, 59, 64, 75, 89, 90, 106, 108, and 112). Glycines 23, 47, 53, 75, 89, 108, and 112 were identified on the basis of their two characteristic cross peaks in the COSY spectrum. Of these Gly108 is noticeable because of the very low field shifted H^N resonance at 11.08 ppm. The H^α protons of Gly106 are almost degenerate but could be identified as well. One of the H^N–H^α cross peaks of Gly56 is hidden under the cross peak of Trp20, but identification of the H^α–H^α cross peak verified this assignment. For Gly90 only one H^N–H^α cross peak was observed and the H^α–H^α has not been observed. Only the H^α–H^α cross peak of Gly64 was observed.

Alanines (16 at Sequence Positions 3, 8, 16, 24, 26, 29, 32, 36, 50, 55, 61, 62, 73, 76, 80, and 87). Fifteen of these were identified using TOCSY and COSY to elucidate the cross-peak network. The identification of Ala87 was hampered because the H^α resonance coincides with the water resonance. Ala8 consists of two sets of cross peaks, of which one disappears at higher temperatures (330 K).

Threonines (Nine at Sequence Positions 9, 33, 49, 70, 74, 79, 97, 100, and 104). Eight of the nine H^β–$H^{\gamma 2}$ cross peaks of threonines were unambiguously identified subsequent to the assignment of the alanine H^α–H^β cross peaks. The remaining ninth H^β–$H^{\gamma 2}$ cross peak of Thr3[illegible] has an unusual

Table I: ^{1}H Chemical Shifts in Barwin at pH 4.20 and 310 K Measured in Parts per Million Relative to the Methyl Group Proton Resonance of 4,4-Dimethylsilapentanesulfonate (±0.01 ppm)[a]

residue	H^N	H^α	H^β	others
Glu1				
Gln2	8.48	5.18	2.32, 2.28	H^γ, 2.65
Ala3	7.62	4.38	1.16	
Asn4	8.48	5.37	2.65, 2.61	$H^{\delta 2}$, 7.38, 6.81
Asp5	8.84	4.35	3.19, 2.85	
Val6	9.61	4.29	2.16	$H^{\gamma 1}$, 1.17; $H^{\gamma 2}$, 1.01
Arg7	8.75	4.53	1.85	H^γ, 1.45; H^δ, 3.07; H^ϵ, 7.60
	(8.71	4.53)		
Ala8	9.39	5.93	1.59	
	(9.36	5.79	1.58)	
Thr9	8.53	4.89	4.50	$H^{\gamma 2}$, 1.33
	(8.29	4.85)		
Tyr10	7.59	6.35	*2.69, 2.16*	H^δ, 5.87; H^ϵ, 6.55
	(7.51	6.35		H^δ, 5.87; H^ϵ, 6.51)
His11	8.56	4.51		$H^{\delta 2}$, 4.97; $H^{\epsilon 1}$, 8.58
	(8.63	4.50		$H^{\delta 2}$, 5.02; $H^{\epsilon 1}$, 8.56)
Tyr12	8.89	5.67	2.89	H^δ, 7.16; H^ϵ, 6.21
				(H^δ, 7.13; H^ϵ, 6.18)
Tyr13	8.70	4.64	3.55	H^δ, 7.56; H^ϵ, 6.81
	(8.67	4.61)		
Arg14	8.04	4.89	1.59	H^γ, 2.00; H^δ, 3.28
Pro15		3.07	–0.59, 1.12	H^γ, 0.92
Ala16	7.96	3.11	1.26	
	(7.94	3.10)		
Gln17	8.06	4.11	2.10	H^γ, 2.56
	(8.01	4.11)		
Asn18	7.46	5.00	*3.11, 2.32*	$H^{\delta 2}$, 6.85, 7.11
Asn19	8.09	4.54	*3.32, 3.01*	$H^{\delta 2}$, 7.78, 6.95
Trp20	9.03	3.55	3.34, 3.10	$H^{\delta 1}$, 7.11; $H^{\epsilon 1}$, 10.25; $H^{\epsilon 3}$, 7.29; $H^{\eta 2}$, 7.02; $H^{\zeta 2}$, 7.37; $H^{\zeta 3}$, 6.48
Asp21	7.89	5.30	*2.86, 3.53*	
Leu22	8.22	4.07	1.39	H^γ, 1.39; H^δ, 0.98, 0.35
Gly23	8.43	4.38, 3.68		
Ala24	7.34	4.65	1.77	
Pro25		4.35	2.51, 2.08	H^γ, 2.36; $H^{\delta 1}$, 4.01; $H^{\delta 2}$, 4.07
Ala26	8.46	4.37	1.57	
Val27	7.98	4.22	2.47	$H^{\gamma 1}$, 1.48; $H^{\gamma 2}$, 1.39
Ser28	8.53	4.07	*4.18, 3.94*	
Ala29	8.10	4.35	1.50	
Tyr30	9.37	4.51	*3.08, 4.03*	H^δ, 7.26; H^ϵ, 6.88
Cys31	7.66	4.96	3.04	
Ala32	8.35	3.71	1.48	
Thr33	6.75	3.35	1.54	$H^{\gamma 2}$, 0.17
Trp34	6.34	4.67	*2.84, 3.44*	$H^{\delta 1}$, 7.36; $H^{\epsilon 1}$, 10.26; $H^{\epsilon 3}$, 7.51; $H^{\eta 2}$, 7.07; $H^{\zeta 2}$, 7.48; $H^{\zeta 3}$, 6.74
Asp35	8.37	4.99	3.12, 2.39	
Ala36	8.55	4.37	1.62	
Ser37	7.98	4.42	*4.11, 3.89*	
Lys38	7.12	4.24	1.74, 1.18	
Pro39		4.96	*2.12, 3.03*	H^γ, 2.63, 2.23; H^δ, 3.90, 3.42
Leu40	9.25	4.09	*1.81, 1.94*	H^γ, 1.48; H^δ, 1.08, 1.04
Ser41	8.90	3.89	3.94, 3.02	
Trp42	7.22	4.29	*3.44, 3.78*	$H^{\delta 1}$, 7.40; $H^{\epsilon 1}$, 10.00; $H^{\epsilon 3}$, 7.37; $H^{\eta 2}$, 7.12; $H^{\zeta 2}$, 7.65; $H^{\zeta 3}$, 6.84
Arg43	8.71	4.28	2.39	H^γ, 2.05
Ser44	8.39	3.53	*2.34, 2.03*	
Lys45	6.67	3.49	*2.05, 1.15*	H^γ, 0.78, –0.27; H^δ, 0.95, 0.00; H^ϵ, 2.39
Tyr46	7.69	5.18	*2.49, 3.47*	H^δ, 6.94; H^ϵ, 6.82
Gly47	9.17	4.18, 3.83		
Trp48	6.75	5.71	2.90, 2.98	$H^{\delta 1}$, 7.56; $H^{\epsilon 1}$, 10.66; $H^{\epsilon 3}$, 6.90; $H^{\eta 2}$, 6.82; $H^{\zeta 2}$, 7.80; $H^{\zeta 3}$, 7.04
	(8.86	5.67)		
Thr49	8.54	5.34	3.78	$H^{\gamma 2}$, 0.87
	(8.57	5.29)		
Ala50	9.40	5.07	1.50	
	(9.29	5.07)		
Phe51	8.51	5.02	3.07, 2.84	
Cys52	7.82	4.28	3.19	
	(7.74	4.30)		
Gly53	8.06	3.95, 4.04		
Pro54				
Ala55	7.13	5.03	1.51	
Gly56	9.03	4.61, 3.55		
Pro57		4.44	*1.52, 2.13*	H^γ, 1.69; H^δ, 2.72, 3.03
Arg58	7.88	5.03	*1.99, 1.80*	
Gly59	8.84	3.65, 4.19		
Gln60	9.33	3.45	*1.65, 1.53*	$H^{\gamma 1}$, 1.34; $H^{\gamma 2}$, 0.63; $H^{\epsilon 2}$, 6.47, 6.35
Ala61	8.10	4.05	1.49	
Ala62	7.40	4.14	1.55	
Cys63	7.43	4.26	*3.68, 3.26*	

Table I (Continued)

residue	H^N	H^α	H^β	others
Gly64		4.73, 3.77		
Lys65	7.88	4.58	*2.25, 2.35*	H^γ, 1.99; H^δ, 1.81, 2.53; H^ϵ, 3.14; H^ζ, 7.59
Cys66	8.85	5.37	2.84, 2.53	
Leu67	8.76	4.89	1.12	H^γ, 0.85; H^δ, 0.20, –0.41
Arg68	9.35	4.92	*1.67, 1.97*	H^γ, 1.43, 2.50; H^δ, 3.16, 3.11; H^ϵ, 7.02
Val69	9.63	4.87	2.02	$H^{\gamma 1}$, 0.90; $H^{\gamma 2}$, 0.82
Thr70	9.01	5.24	3.89	$H^{\gamma 2}$, 1.08
Asn71	9.29	5.37	*2.51, 3.60*	$H^{\delta 2}$, 8.04, 7.71
Pro72		4.52	*2.20, 2.45*	H^γ, 2.04; $H^{\delta 1}$, 4.29; $H^{\delta 2}$, 4.59
Ala73	7.64	4.40	1.67	
Thr74	6.95	4.77	4.55	$H^{\gamma 2}$, 1.21
Gly75	8.82	4.39, 3.65		
Ala76	7.59	4.44	1.61	
Gln77	8.43	5.79	1.94, 1.94	H^γ, 2.51, 2.40; $H^{\epsilon 2}$, 7.59, 6.78
Ile78	8.79	4.59	1.76	$H^{\gamma 1}$, 1.86, 1.54; $H^{\gamma 2}$, 0.89; H^δ, 1.24
Thr79	8.23	5.31	3.88	$H^{\gamma 2}$, 0.28
Ala80	9.29	5.11	1.08	
Arg81	9.42	4.76	1.74, 1.64	H^γ, 1.76, 1.62; H^δ, 3.16, 3.37; H^ϵ, 7.30; H^η, 6.94
Ile82	9.23	4.30	2.21	$H^{\gamma 2}$, 1.11; H^δ, 0.48
Val83	8.53	4.45	2.21	H^γ, 1.03, 1.17
	(8.51	4.45	2.21	H^γ, 1.03, 1.20)
Asp84	7.85	5.57	2.77, 2.57	
Gln85	8.73	5.27	1.87, 1.87	H^γ, 2.27; $H^{\epsilon 2}$, 6.71, 6.49
	(8.80	5.27)		
Cys86	7.05	5.08	*2.82, 3.55*	
	(7.02	5.13)		
Ala87	8.71	4.77	1.38	
Asn88	7.74	4.87	*3.10, 2.65*	
Gly89	8.14	3.87, 4.07		
Gly90	7.95	4.03		
Leu91	8.19	4.89		H^γ, 1.71; H^δ, 0.94, 0.91
Asp92	7.22	5.18	2.91, 3.79	
Leu93	8.54	4.71		H^γ, 1.80; H^δ, –0.02, 0.03
Asp94	7.90	3.93	2.35, 2.71	
	(7.88	3.93)		
Trp95		4.08	3.05, 2.76	$H^{\delta 1}$, 7.09; $H^{\epsilon 1}$, 9.92; $H^{\epsilon 3}$, 6.49; $H^{\eta 2}$, 6.75; $H^{\zeta 2}$, 7.20; $H^{\zeta 3}$, 6.46
Asp96	7.08	4.64		
Thr97	8.98	4.42	4.64	$H^{\gamma 2}$, 1.34
	(9.01	4.42)		
Val98	7.39	4.50	2.54	$H^{\gamma 1}$, 1.00; $H^{\gamma 2}$, 1.17
	(7.36	4.49)		
Phe99	9.52	3.71	*3.07, 3.29*	H^δ, 7.18; H^ϵ, 7.43; H^ζ, 6.96
Thr100	7.98	3.72	3.50	$H^{\gamma 2}$, 0.12
	(8.01	3.71)		
Lys101	6.62	4.15	1.93	H^γ, 1.19, 1.44; H^δ, 1.61, 1.49; H^ϵ, 3.07; H^ζ, 7.17
	(6.61	4.15)		
Ile102	6.97	4.67	1.99	$H^{\gamma 1}$, 1.13, 1.00; $H^{\gamma 2}$, 0.70; H^δ, 0.56
Asp103	7.67	4.89	3.20, 2.71	
Thr104	7.77	3.95	4.18	$H^{\gamma 2}$, 1.28
Asn105	8.26	5.08	3.16, 3.00	$H^{\delta 2}$, 7.71, 6.97
	(8.23	5.08)		
Gly106	7.57	4.16, 4.21		
Ile107	7.45	4.01	1.94	$H^{\gamma 1}$, 1.54, 1.36; $H^{\gamma 2}$, 1.01; H^δ, 0.94
Gly108	11.08	4.13, 3.48		
Tyr109	9.36	4.44	*3.59, 3.25*	H^δ, 7.07; H^ϵ, 6.68
Gln110	7.43	4.09		
Gln111				
Gly112	8.41	4.54, 3.95		
His113	7.86	5.54	3.58, 3.14	$H^{\delta 1}$, 8.81; $H^{\epsilon 1}$, 7.11
	(7.87	5.52)		
Leu114	9.67	4.72	1.45, 1.44	H^γ, 1.46; H^δ, 0.72, 0.41
Asn115	8.74	5.51	2.80, 2.70	
Val116	9.57	5.30	2.51	$H^{\gamma 1}$, 0.77; $H^{\gamma 2}$, 0.87
	(9.55	5.29)		
Asn117	8.79	5.72	*3.30, 2.68*	$H^{\delta 2}$, 7.56, 6.77
Tyr118	8.95	6.29	*3.05, 2.73*	H^δ, 6.89; H^ϵ, 6.91; H^η, 10.68
Gln119	8.40	5.41	*2.10, 2.19*	H^γ, 2.44; $H^{\epsilon 2}$, 7.67, 6.88
Phe120	9.46	4.95	*3.38, 3.05*	H^δ, 7.46; H^ϵ, 7.10; H^ζ, 6.14
Val121	8.56	4.84	2.20	$H^{\gamma 1}$, 0.55; $H^{\gamma 2}$, 0.89
Asp122	8.50	4.56	2.79, 2.79	
Cys123	9.05	4.29	*3.05, 3.26*	
Arg124	9.35	3.99	2.50, 2.08	H^γ, 1.80, 1.71; H^δ, 3.28; H^ϵ, 7.22
Asp125	7.95	4.47	*3.03, 2.67*	

[a] Assignments for Glu1, Pro54, and Gln111 have not been found. Chemical shift values for β-methylene protons and γ-methyl protons of valines which have been stereospecifically assigned are written in italics. The first chemical shift thus listed is $H^{\beta 2}$,$H^{\gamma 1}$ and the second $H^{\beta 3}$, $H^{\gamma 2}$, respectively, for β-methylene protons and γ-methyl groups in valines. Numbers in parentheses are for the second set of resonances (see text).

high-field chemical shift of the H^{β} proton (1.54 ppm) and was only correctly assigned in the sequential assignment process. The full assignment of Thr9, Thr70, Thr97, Thr100, and Thr104 was accomplished in TOCSY and COSY of barwin dissolved in 1/19 $^2H_2O/H_2O$. The H^{α}, H^{β}, and $H^{\gamma 2}$ cross-peak network for the rest of the threonines could easily be identified in TOCSY and COSY spectra of barwin dissolved in ^2H_2O, and a comparison with the H_2O spectra was used to identify the H^N resonances.

Valines (Seven at Sequence Positions 6, 27, 69, 83, 98, 116, and 121). The characteristic COSY H^{β}–H^{γ} methyl cross peaks were immediately found for six of the valines. These valine cross peaks are well separated, and the distinction between these and the isopropyl couplings of leucine was achieved from the combined analysis of COSY and TOCSY. For the remaining valine, Val83, the two methyl group resonances are present twice in the spectra, and therefore the assignment of this was fully accomplished by the sequential assignment.

Isoleucines (Four at Sequence Positions 78, 82, 102, and 107). Three sets of isoleucine ethyl cross peaks were observed in COSY (Figure 2), whereas the remaining set of Ile82 was weak, probably due to degeneracy of the $H^{\gamma 1}$ methylene protons. For all four isoleucines the connections to the rest of their spin systems were established on the basis of a TOCSY cross peak between the $H^{\gamma 2}$ and the H^{δ} methyl groups. The connection from the $H^{\gamma 2}$ methyl group to H^N, H^{α}, and H^{β} were obtained from COSY and TOCSY.

Leucines (Six at Sequence Positions 22, 40, 67, 91, 93, and 114). Once the valine spin systems were assigned, the remaining isopropyl cross peaks were assigned to leucines (Figure 2). Several of these resonances are significantly shifted compared to the typical values. Since TOCSY spectra were of no help for the full assignment of the leucines, NOESY was used to identify potential H^{α}–H^{δ} connectivities (Redfield & Dobson, 1987). For Leu22, Leu40, Leu67, and Leu114 the spin systems were assigned uniquely; however, for the remaining two leucines assignments were achieved in the sequential assignment process. One particular problem with Leu91 and Leu93, and several spin systems in that region of the protein sequence, arose because the intensities of the H^N–H^{α} cross peaks were very low.

AMX Spin Systems (45 Residues Totally). AMX spin systems were identified in COSY spectra of barwin dissolved in ^2H_2O. They were distinguished from other spin systems primarily by the chemical shift position of the H^{β} protons and by recognition of the characteristic cross-peak patterns (Hyberts et al, 1987); however, a few exceptions to these generel criteria were observed.

Aromatic Residues (Seven Tyrosines at Sequence Positions 10, 12, 13, 30, 46, 109, and 118; Five Tryptophans at 20, 34, 42, 48, and 95; Three Phenylalanines at 51, 99, and 120). The assignment of the spin systems of the benzenoide part of the aromatic side chains in phenylalanines, tryosines, and tryptophans was obtained from the set of COSY, relayed COSY, and TOCSY spectra in which resonances of all the aromatic protons were identified. The connectivity of the benzenoide part of the spin systems of the five tryptophans to the $H^{\epsilon 1}$ and the $H^{\delta 1}$ of the indole ring was in both cases obtained from the NOE effects between the $H^{\epsilon 1}$ and the $H^{\zeta 2}$. The cross peak $H^{\epsilon 1}$–$H^{\delta 1}$, which is located in a unique region of the spectrum, was identified for all five tryptophans in the NOESY spectrum; however, the $H^{\epsilon 1}$–$H^{\delta 1}$ COSY cross peak of Trp95 was not observable. Only two of the three aromatic ring system assignments of phenylalanine are reported in Table I since the last potential phenylalanine cross-peak network (6.95, 7.30, 6.73) is weak and not observed to be connected by NOEs to the aliphatic part of Phe51. The assignment is therefore made tentatively and based on exclusion.

The connectivities between the aromatic and the aliphatic spin systems of the rest of the amino acids were obtained in all cases from the NOEs between the H^{δ}s and the H^{β}s and in most cases also between the H^{α} or the H^N, respectively, and the H^{δ} of the spin systems. In Tyr118 the chemical shifts of the H^{δ} and H^{ϵ} protons are almost equivalent; thus, the aromatic part of this spin system was established only when the aliphatic part of the spin system was sequentially assigned. In Tyr10, Tyr12, and Tyr13 most of the aromatic and aliphatic protons have two set of resonances. Some of these aromatic resonances are shifted significantly compared to the typical values, especially Tyr10 and Tyr12. The structure calculation presented in the following paper (Ludvigsen & Poulsen, 1992) has shown that the only possible assignment of a resonance at 10.68 ppm was the hydroxyl group of Tyr118 as based on the NOESY cross peaks at this unique position. Tyr118 is in fact also the only tyrosine that is buried in the interior of the protein.

Histidines (Two at Sequence Positions 11 and 113). Only one of the histidines has been fully assigned, His113. The histidine cross peak $H^{\delta 2}$–$H^{\epsilon 1}$ in COSY is characteristic, and therefore a similar cross peak at (4.97, 8.58) ppm was tentatively assigned to His11. Further support for this was obtained from an NOE between the H^{α} proton in His11 and this $H^{\delta 2}$ proton. All identified protons of His11 have two sets of resonances in the spectra similar to many other protons of spin systems in the sequence from Arg7 to Arg14.

Nonaromatic Residues with AMX Spin Systems (10 Aspartates at Sequence Positions 5, 21, 35, 84, 92, 94, 96, 103, 122, and 125; 8 Asparagines at 4, 18, 19, 71, 88, 105, 115, and 117; 6 Cystines at 31, 52, 63, 66, 86, and 123; 4 Serines at 28, 37, 41, and 44). Most of these spin systems are fully assigned (Table I), the exceptions being Asp64 and Cys52. For several of the asparagines assignments of the $H^{\delta 2}$ amide protons were accomplished (Asn4, Asn18, Asn19, Asn71, Asn105, Asn117) by the finding of intense NOEs between H^{β} and $H^{\delta 2}$ protons. The intense cross peaks between the two $H^{\delta 2}$ protons were observed only in NOESY spectra of barwin dissolved in 1/19 $^2H_2O/H_2O$. Ser28 and Ser37 were initially identified as potential serine spin systems due to the low-field resonances of the H^{β} protons. Ser41 and Ser44, however, could not be identified in this way. Again, the sequential assignment process was used as the ultimate identification for several of these spin systems.

Long Side Chain Spin Systems. Initially these spin systems were grouped into one class partly on the basis of chemical shift values of the H^{β} protons, partly on the cross-peak patterns of the H^{α}–H^{β} cross peaks which are distinct from those of the AMX spin systems, and of course on the identification of additional resonances belonging to the spin system.

Pyroglutamate and Glutamines (Glp1; Eight Glutamines at Sequence Positions 2, 17, 60, 77, 85, 110, 111, and 119). The spin systems of Glp1 and Gln111 were not observed in any of the spectra. For the remaining glutamines several could be pointed out as potential candidates for either glutamine or pyroglutamate spin systems and others could be fully assigned. Full assignment was obtained for Gln60, Gln77, Gln85, and Gln119. The resonances of Gln60 are shifted compared to the typical glutamine resonance values, but the presence of the $H^{\epsilon 2}$ resonances supported assignment of this spin system. The unusual shifts are probably caused by Tyr30 that has many NOEs to Gln60. The Gln2 and Gln17 were assigned to either glutamines or pyroglutamate due to the

characteristic chemical shift of the H^{β} and H^{γ} protons.

Arginines (Seven at Sequence Positions 7, 14, 43, 58, 68, 81, and 124). Arg7, Arg14, Arg68, Arg81, and Arg124 were unambiguously assigned on the basis of TOCSY and COSY. All resonances of these five arginines are close to the typical values. For Arg43 and Arg58 the H^N, H^{α}, and H^{β} resonances were assigned; thus, their identification relied on sequential assignments.

Lysines (Four at Sequence Positions 38, 45, 65, and 101). Three of the four lysines were unambiguously assigned, only Lys38 is only assigned with respect to the H^N, H^{α}, and H^{β} resonances. The resonances of Lys45 are shifted considerably.

Prolines (Six at Sequence Positions 15, 25, 39, 54, 57, and 72). Pro25, Pro72, and Pro57 were assigned immediately. Pro15 and Pro39 both have atypical chemical shifts and were identified by the sequential assignment. No resonances were observed for Pro54.

Sequential Assignment. The sequential assignment was based on the analysis of NOESY spectra with a mixing time of 150 ms of barwin dissolved in ^2H_2O and in 1/19 ^2H_2O/H_2O, respectively. The general approach was first to analyze the most intense cross peaks in the fingerprint region and the area in the spectra with potential H^N–H^N cross peaks. The result of the sequential assignments is given in Figure 3, using the standard notation (Wüthrich, 1986). The fingerprint region of the NOESY spectrum is dominated by many intense $d_{\alpha N}(i,i+1)$ NOEs, which were easily assigned. By these the sequential stretches from Gln2 to Thr9, from Trp48 to Cys52, from Ala55 to Gly59, from Gly64 to Pro72, from Ala76 to Val83, from Asp84 to Ala87, and from Asn115 to Val121 were sequentially assigned (Figure 4). For prolines the $d_{\alpha\delta}(i,i+1)$ connectivities were used. Once it was realized that the residues from 7 to 13 all possessed double peaks, the stretch from 2 to 9 could be extended up to Tyr13. By analysis of the H^N–H^N region (Figure 5) and including the remaining $d_{\alpha N}(i,i+1)$ and $d_{\beta N}(i,i+1)$ connectivities the sequential assignment was accomplished for most of the remaining spin systems. Thus, stretches from Gln2 to Tyr13, from Pro15 to Pro39, from Leu40 to Gly53, from Ala55 to Asn88, from Asp96 to Gln110, and from Gly112 to Asp125 were sequentially assigned. The spin system assigned for Arg14 could not be connected to its neighbors; however, several indications for this sequential assignment were identified. Furthermore, the sequential assignment of this residue was obtained by exclusion since this arginine was the only residue not assigned at this stage. One NOE is present between the H^{α} proton of Arg14 and potential H^{δ} resonance of Pro15. Furthermore, the resonances of H^N and H^{α} in Tyr12, Tyr13, and Arg14 are all weak due to large line widths. No NOEs were found connecting Pro39 and Leu40, and as mentioned previously the spin systems of Pro54, Gln111, and Glu1 have not been identified. The remaining gap in the sequential assignment was between Gly89 and Trp95. Trp95 was assigned when the other four tryptophans unambiguously had been sequentially assigned. However, no sequential NOEs were found for this residue, partly because no amide proton was identified for this spin system. Weak sequential NOEs connect the stretch Gly89, Gly90, and Leu91, and sequential NOEs closed the gap to Asp94. It is characteristic that sequential NOEs were almost all weak in the stretch between Gly89 and Asp94 and therefore contained little structural information.

Stereospecific Assignments. Stereospecific assignment for protons of 26 of the H^{β} methylene groups and 6 of the H^{γ} methyl groups of valine spin systems was obtained by identifying the staggered rotamer conformation (Table I) using NOESY and COSY. In some cases no conclusion concerning the stereospecific assignment and the determination of the χ^1 angle could be obtained. Typically this situation was encountered when NOEs and $^3J_{\alpha\beta}$ coupling constants appeared to be a result of averaging between two or more of the staggered conformations.

Secondary Structure. The measurements of coupling constants and the characterization of hydrogen exchange (Figure 3) were used in conjuction with sequential NOEs and some long-range NOEs to characterize most of the secondary structure of barwin. The protein is dominated by a large antiparallel β-sheet as demonstrated by many intense $d_{\alpha\alpha}$ long-range NOEs (Figure 6). This β-sheet includes the residues Gln2–Thr9, Lys65–Asn71, Gln77–Arg81, and His113–Val121 (Figure 7). Between Asn71 and Gln77 there is a small well-defined loop starting with Pro72 and ending with Ala76 which apparently is part of the β-sheet despite its small $^3J_{H^NH^{\alpha}}$. Residues Asp5 and Val6 make a β-bulge, as indicated by the observation of the positive ϕ angle of Asp5. Many long-range NOEs have been found between the four strands of the β-sheet. The stretch from Tyr10 to Tyr13 has sequential NOEs and $^3J_{H^NH^{\alpha}}$ coupling constants typical of β-sheets, but no corresponding strand has been identified at this stage (see succeeding paper). Two sequence strands—Asp84–Ala87 and Trp48–Cys52—are connected by cross-strand NOEs, suggesting the existence of a short parallel β-sheet (Figure 7).

The structure calculation described in the succeeding paper (Ludvigsen & Poulsen, 1992) suggests that the strand from Tyr10 to Tyr13 forms a parallel β-strand with the strand Gly90–Asp94; however, no cross-strand NOEs were observed between the two strands. The strand Gly90–Asp94 forms an antiparallel β-sheet to the strand Trp48–Cys52. Thus, a second four-stranded β-sheet was identified as a result of the structure calculation; however, the absence of several cross-strand NOEs prevented the identification of this element of secondary structure in the first stage of analysis.

There are only short α-helices in barwin. The first α-helix starts at residue Tyr30 and ends at Lys38, with an irregularity at Asp35 which has a ϕ angle at $-120° \pm 40°$ as seen from the large $^3J_{H^NH^{\alpha}}$. After Pro39, which is in trans conformation, a second very short α-helix begins at Leu40 and ends at Tyr46. This α-helix is well-defined with the sequential NOEs and slow amide proton exchange for the residues Arg43, Ser44, and Lys45. From Thr97 to approximately Asp103 is the third short α-helix with sequential NOEs and $^3J_{H^NH^{\alpha}}$ coupling constants typical of α-helices with the exception of the intense $d_{\alpha N}(98,99)$. A fourth α-helix that could not be derived directly from the sequential NMR information was suggested from the structure calculations between residues 106 and 111 (Ludvigsen & Poulsen, 1992).

Additional secondary structure in barwin was observed mainly as turns and loops. Residues Asn18–Asp21 participate in a turn III′ as indicated by the positive ϕ angles found for Asn19 and Trp20. Residues Asp21–Ala24 form a type I turn; Pro25 is in trans conformation indicated by the intense $d_{\alpha\delta}(24,25)$ NOE. Pro25 is followed by a turn II with a positive ϕ angle for Ser28. The sequence from Gly53 to Gly64 has four preserved glycines (Svensson et al., 1992), suggesting the presence of turns in this part of the protein; however, no turns in this part of the sequence were identified by the NMR analysis. The amino acid sequence ends with a turn where Arg124 has a positive ϕ angle.

Cystine Bridges. NOEs were identified between the protons of Cys123 and Cys66 and thus indicate one of the three cystine bonds. From the secondary structure evaluation (Figure 3) of the parallel β-sheet the geometric arrangement allows Cys86

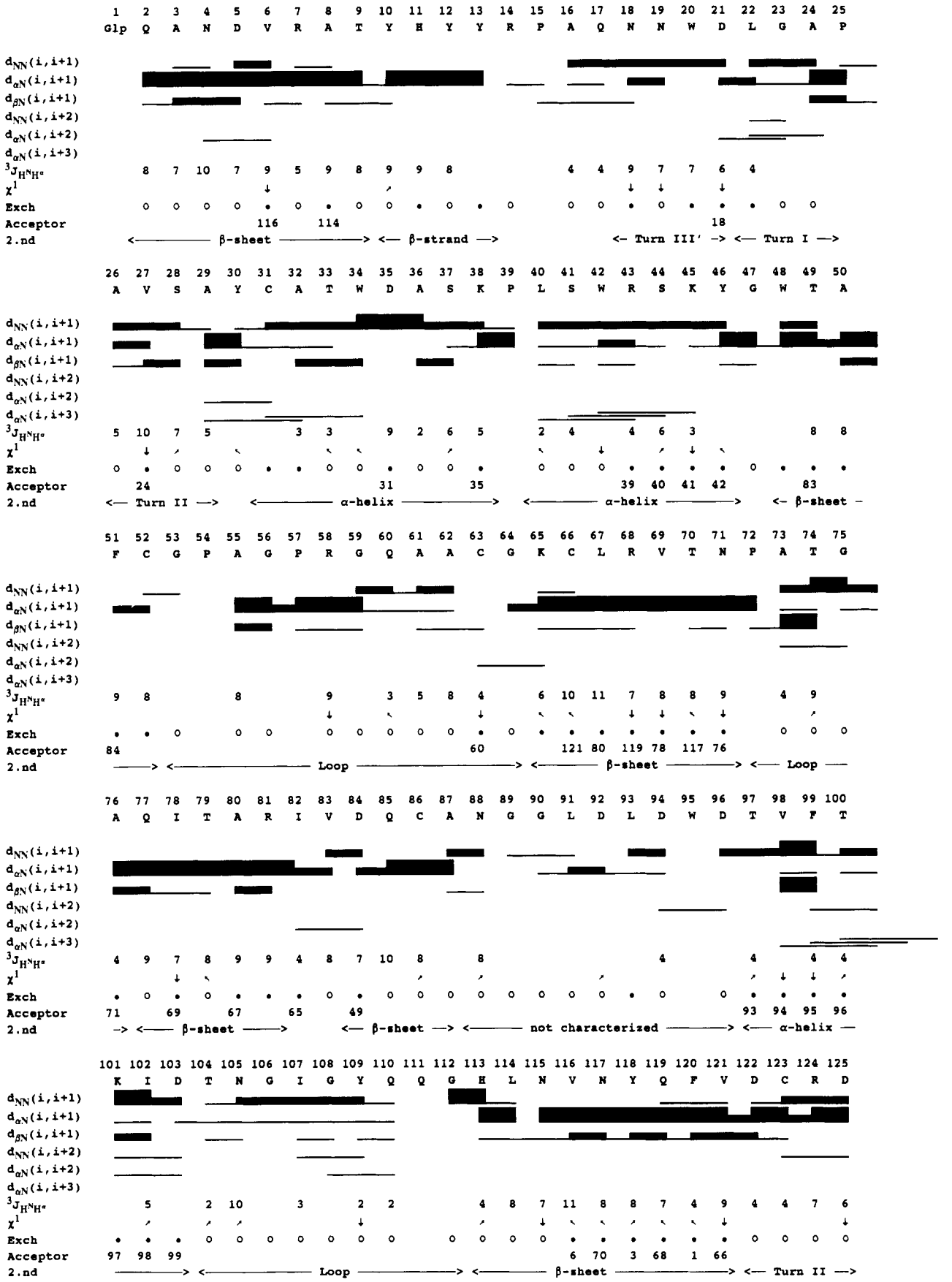

FIGURE 3: Overview of the sequential NOEs assigned for barwin as well as $^3J_{H^NH^\alpha}$ coupling constants, exchange rates (Exch) of amide protons, acceptor of hydrogen bonding indicated by slow exchange (Acceptor), the side-chain conformation (χ^1), and the assignment of secondary structure (2.nd). The thickness of the bars representing the sequential NOE reflects the intensity classification made (see text). Thick bars are thus representative of strong NOEs, medium bars of medium NOEs, and thin bars of weak NOEs. Coupling constants are measured in hertz. The side-chain conformations with respect to the dihedral angle χ^1 are listed using arrows. Arrows pointing down represent a χ^1 of 180° ± 60°, pointing up to the right represent 60° ± 60°, and pointing up to the left represent −60° ± 60°. Amide protons observable after 24 h at 310 K at pH 4.20 in the COSY spectrum of the protein dissolved in ^2H_2O were categorized as slow (●) and those that were not observable as fast (○).

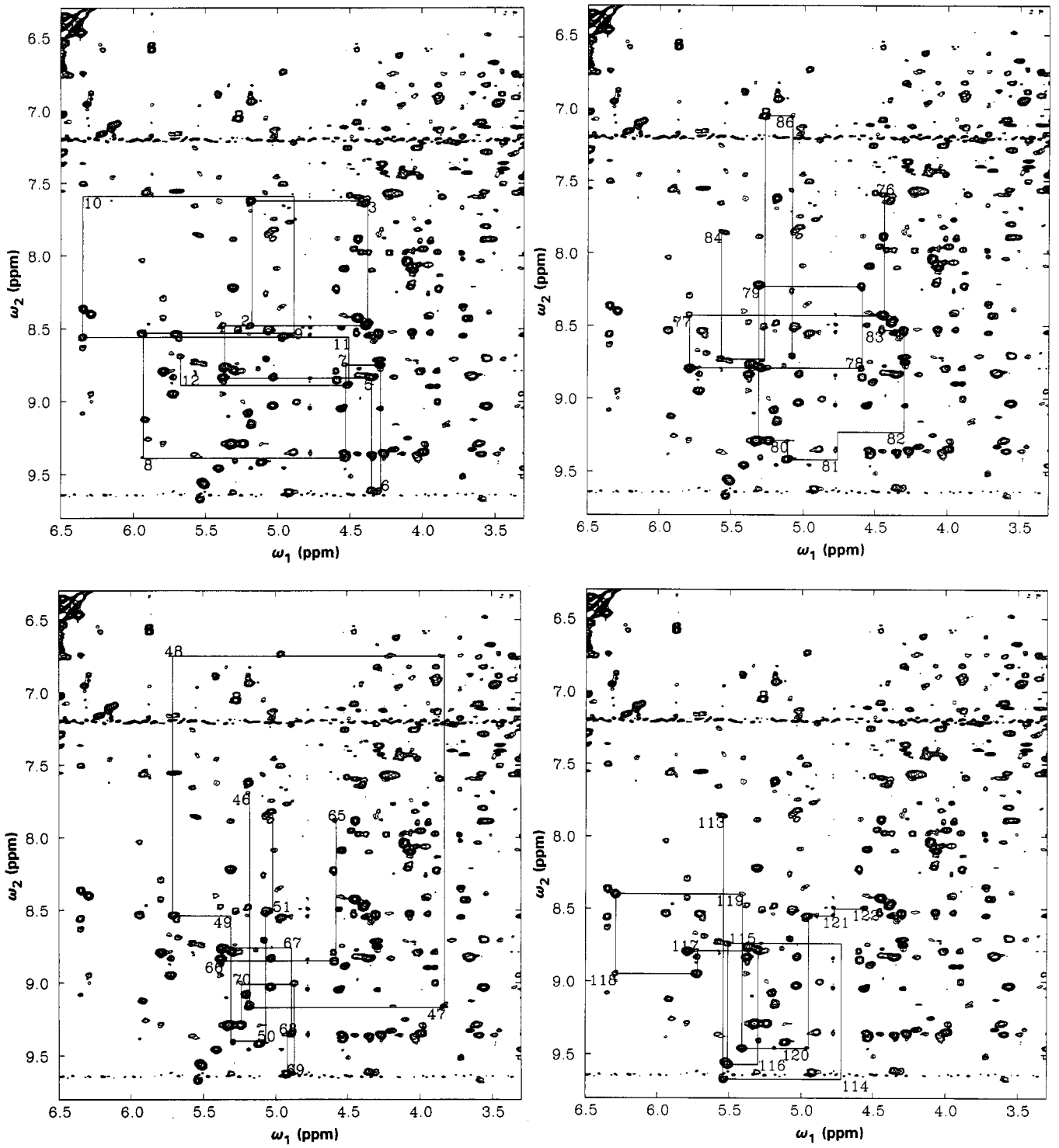

FIGURE 4: NOESY spectrum of the fingerprint region of barwin. The spectrum was acquired at 310 k, pH 4.20, of barwin dissolved in 1/19 $^2H_2O/H_2O$. The spectrum was processed as described in the text. (a, top left) Sequential pathways of $d_{\alpha N}(i,i+1)$ of residue Gln2–Tyr13. The numbers indicate the residue position in the sequence. Note that intra-H^N–H^α NOEs are not seen for all residues. (b, bottom left) Residues Tyr46–Cys52 and Lys65–Asn71; (c, top right) Ala76–Ala87; (d, bottom right) His113–Asp122.

and Cys52 to have a cystine bridge. Since no free cysteine exists in barwin, the last cystine bridge has to be between Cys31 and Cys63. These findings were confirmed by plasma desorption mass spectrometry (Svensson et al., 1992).

DISCUSSION

The secondary structure of barwin as determined here was based primarily on the complete sequence-specific assignment of 122 of 125 amino acid spin systems. For 104 of these it was possible to obtain full and unambiguous assignment of the spin systems, and only 18 systems were only partially assigned. Furthermore, the secondary structure determination relied on the accurate measurement of the H^N–H^α coupling constant for 87 residues of a total of 107 potential residues for which the measurement might have been possible and a total 359 sequential and 36 long-range NOEs.

The resulting secondary structure outlined in this study primarily consists of the four-stranded antiparallel β-sheet, the two short parallel strands, three short α-helices, and four turns. These secondary structures account for 37 of the 49 amides observed to have slow amide exchange. Most of the remaining amide hydrogens also observed to have slow

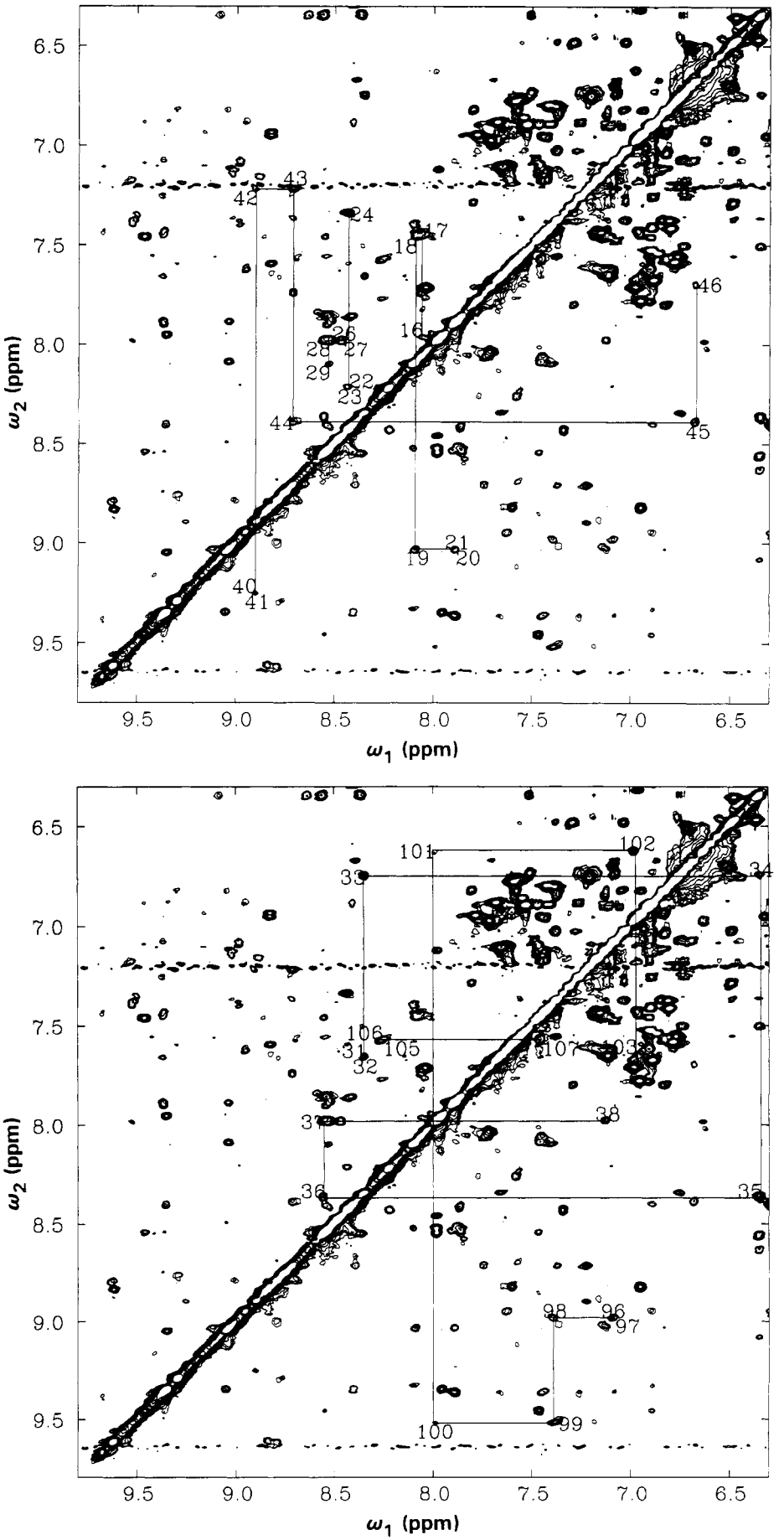

FIGURE 5: Same spectrum as in Figure 4 of the H^N–H^N region. Sequential pathways of $d_{NN}(i,i+1)$ are shown with lines. (a, top) From residue Ala16 to Asp21, from Leu22 to Ala24, from Ala26 to Ser28, and from Leu40 to Tyr46; (b, bottom) from Cys31 to Lys38, from Asp96 to Asp103, and from Asn105 to Ile107.

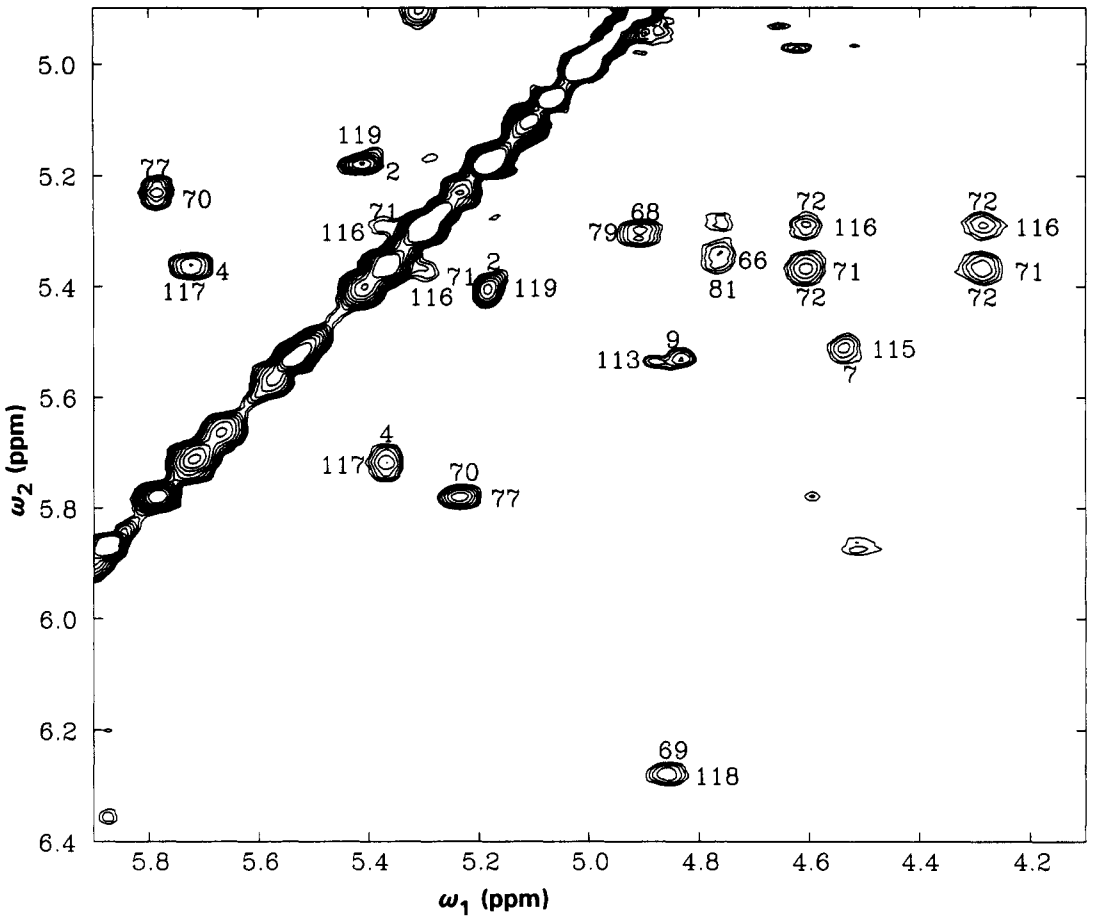

FIGURE 6: NOESY spectrum of barwin dissolved in 99.96% ^2H_2O at 310 K and pH 4.20. The region shows several intense $d_{\alpha\alpha}$ long-range NOEs typical for antiparallel β-sheets. Also, the $d_{\alpha\delta}(i,i+1)$ from Asn71 to Pro72 as well as the cross-strand NOE between Val116 H^{α} and Pro72 $H^{\delta 1}$ and $H^{\delta 2}$ are shown.

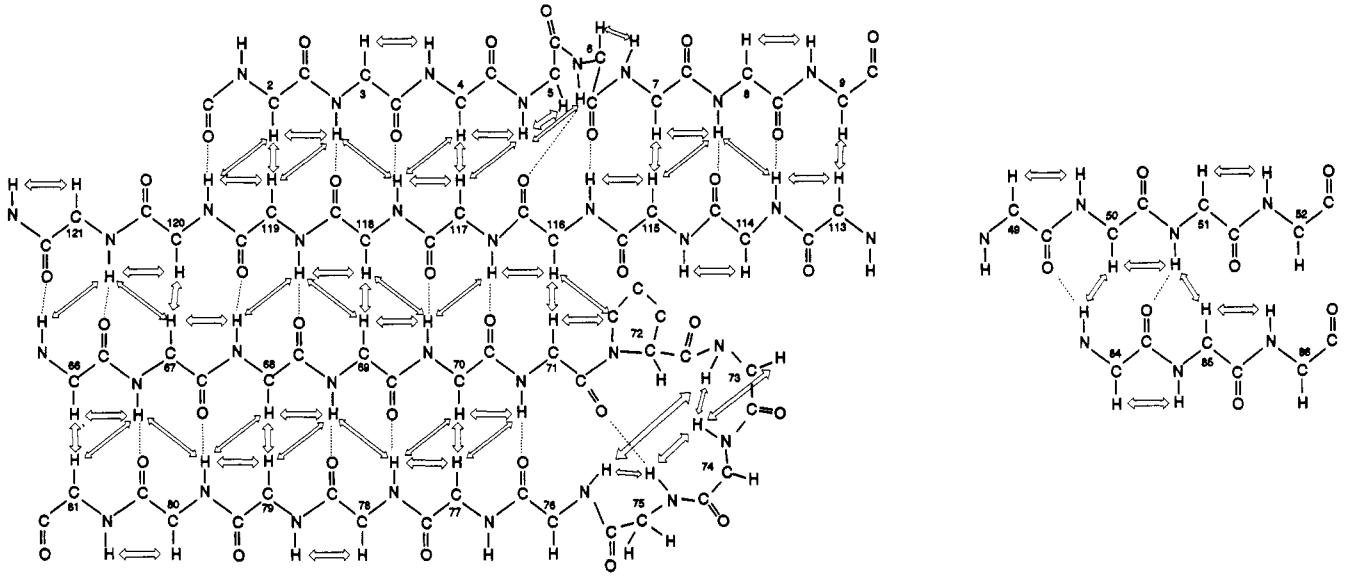

FIGURE 7: Four-stranded antiparallel β-sheet (a, left) of barwin as found by the secondary structure elucidation. NOEs are indicated by arrows. The thickness of the arrows does not indicate the intensity of the involved NOE. The twist of the β-sheets is not indicated by this schematic representation. Dotted lines indicate hydrogen bonds as they are found in the calculated structures presented in the following paper. (b, right) Small parallel β-sheet in barwin.

exchange are most likely involved in secondary structure arrangements as well. In the following paper (Ludvigsen & Poulsen, 1992) the hydrogen bonds and their associated secondary structures will be discussed in more detail on the basis of the full structure determination.

The spectral indications that two conformations of barwin exist at the conditions used were all assigned to amino acid residues in regions of the protein sequence associated with the four ill-defined β-strands in the secondary structure and a confined region in the three-dimensional structure as shown in the succeeding paper (Ludvigsen & Poulsen, 1992). This suggests that the two conformations in the sample represent a local conformational difference. We could exclude the possibility that the observed differences are caused by covalent differences between two forms of the protein present in our samples by studies of plasma desorption mass spectrometry

of trypsin fragments of the protein (Svensson et al., 1992). Observations suggesting dual conformations in other proteins studied by NMR spectroscopy have been reported (Fox et al., 1986; Evans et al., 1987; Chazin et al., 1989). These have been assigned to the existence of the cis/trans isomerism of the peptide bond of prolines. Pro15 is in one of the sequence fragments where double peaks occur; however, the sequential NOEs that could have provided information about the proline peptide bond conformation were not unambiguously identified.

The two conformers were shown to exist in a ratio of 1:3 at the conditions typically used. The assignments and the structure determination reported in this paper are only for the predominant form of these two. The difference between the two structures, however, is most likely subtle and only detectable as chemical shift differences. Measurements of $^3J_{H^NH^\alpha}$ and investigations of sequential NOEs for the two conformers do not indicate differences between the two structures.

The presence of two conformers in barwin has of course hampered the NMR analysis of one particular region of the protein structure by doubling the number of NMR signals. Similarly, other resonances from the very same region caused problems for the work because severe line broadening made these difficult to detect, in particular the resonances of residues Asn88–Asp94. Nevertheless, the present work has provided the basis for the assignment of the NOE spectrum of the protein, and the calculation of the three-dimensional structure of barwin. This work will be presented in the following paper (Ludvigsen & Poulsen, 1992).

ACKNOWLEDGMENT

We thank Pia Mikkelsen for skilled technical assistance and Mogens Kjær and Kim Vilbour Andersen for advice and help with computations. We also thank Jens Christian Madsen for a critical reading of the manuscript. F.M.P. is a member of the Danish Protein Engineering Research Centre (PERC).

REFERENCES

Anil-Kumar, Ernst, R. R., & Wüthrich, K. (1980) *Biochem. Biophys. Res. Commun. 95*, 1–5.

Anil-Kumar, Wagner, G., Ernst, R. R., & Wüthrich, K. (1981) *J. Am. Chem. Soc. 103*, 3654–3658.

Aue, W. P., Bartholdi, E., & Ernst, R. R. (1976) *J. Chem. Phys. 64*, 2229–2246.

Bachmann, P., Aue, W. P., Müller, L., & Ernst, R. R. (1977) *J. Magn. Reson. 28*, 29–39.

Bax, A., & Davis, D. G. (1985) *J. Magn. Reson. 65*, 355–360.

Boyd, J., Dobson, C. M., & Redfield, C. (1983) *J. Magn. Reson. 55*, 170–176.

Braunschweiler, L., & Ernst, R. R. (1983) *J. Magn. Reson. 53*, 521–528.

Braunschweiler, L., Bodenhausen, G., & Ernst, R. R. (1983) *Mol. Phys. 48*, 535–560.

Broekaert, W., Lee, H. I., Kush, A., Chua, N. H., & Raikhel, N. (1990) *Proc. Natl. Acad. Sci. U.S.A. 87*, 7633–7637.

Chazin, W. J., Kördel, J., Drakenberg, T., Thulin, E., Brodin, P., Grundström, T., & Forsén, S. (1989) *Proc. Natl Acad. Sci. U.S.A. 86*, 2195–2198.

Dietrich, W., Rüdel, C. H., & Neumann, M. (1991) *J. Magn. Reson. 91*, 1–11.

Eich, G., Bodenhausen, G., & Ernst, R. R. (1982) *J. Am. Chem. Soc. 104*, 3731–3732.

Evans, P. A., Dobson, C. M., Kautz, R. A., Hatfull, G., & Fox, R. O. (1987) *Nature 329*, 266–268.

Fox, R. O., Evans, P. A., & Dobson, C. M. (1986) *Nature 320*, 192–194.

Griesinger, C., Otting, G., Wüthrich, K., & Ernst, R. R. (1988) *J. Am. Chem. Soc. 110*, 7870–7872.

Hyberts, S. G., Märki, W., & Wagner, G. (1987) *Eur. J. Biochem. 164*, 625–635.

Jeener J., Meier, B. H., Bachmann, P., & Ernst, R. R. (1979) *J. Chem. Phys. 71*, 4546–4553.

Kjær, M., Andersen, K. V., Shen, H., Ludvigsen, S., Vindekilde, D., Sørensen, B., & Poulsen, F. M. (1991) *NATO ASI Series* (Hoch, J. C., Redfield, C., & Poulsen, F. M., Eds.) Plenum, New York.

Lee, H., Broekaert, W. F., & Raikhel, N. V. (1991) *J. Biol. Chem. 266*, 15944–15948.

Ludvigsen, S., & Poulsen, F. M. (1992) *Biochemistry* (third of three papers in this issue).

Ludvigsen, S., Andersen, K. V., & Poulsen, F. M. (1991) *J. Mol. Biol. 217*, 731–736.

Marion, D., & Wüthrich, K. (1983) *Biochem. Biophys. Res. Commun. 113*, 967–974.

Neuhaus, D., Wagner, G., Vašák, M., Kägi, J. H. R., & Wüthrich, K. (1985) *Eur. J. Biochem. 151*, 257–273.

Piantini, U., Sørensen, O. W., & Ernst, R. R. (1982) *J. Am. Chem. Soc. 104*, 6800–6801.

Rance, M., Sørensen, O. W., Bodenhausen, G., Wagner, G., Ernst, R. R., & Wüthrich, K. (1983) *Biochem. Biophys. Res. Commun. 117*, 479–485.

Stanford, A., Bevan, M., & Northcote, D. (1989) *MGG, Mol. Gen. Genet. 215*, 200–208.

States, D. J., Haberkorn, R. A., & Ruben, D. J. (1982) *J. Magn. Reson. 48*, 286–292.

Svensson, B., Svendsen, I., Højrup, P., Roepstorff, P., Ludvigsen, S., & Poulsen, F. M. (1992) *Biochemistry* (first of three papers in this issue).

Wagner, G. (1983) *J. Magn. Reson. 55*, 151–156.

Wagner, G., & Zuiderweg, E. R. P. (1983) *Biochem. Biophys. Res. Commun. 113*, 854–860.

Wüthrich, K. (1986) *NMR of Proteins and Nucleic Acids*, Wiley, New York.